Third Quarterly Progress Report
NO1-DC-6-2111

The Neurophysiological Effects of Simulated Auditory Prosthesis Stimulation

C.A. Miller, P.J. Abbas, J.T. Rubinstein, and A.J. Matsuoka

Department of Otolaryngology - Head and Neck Surgery
and
Department of Speech Pathology and Audiology

University of Iowa
Iowa City, IA 52242

July 28, 1997

Contents

List of Figures

1 Introduction

Since their introduction as a clinically proven auditory prosthesis, cochlear implants have undergone design enhancements yielding considerable improvement in users' speech perception scores. Nonetheless, current speech processing and stimulation strategies are limited in their ability to transfer information to the auditory nerve and central nervous system due, in part, to spatial and temporal interactions occurring at the level of the auditory nerve. In this research project, our approach is to better understand these limitations and provide information leading toward the development of new stimulation strategies. We are using both computer simulations and experimental findings to:

1. Characterize the fundamental spatial and temporal properties of intracochlear stimulation of the auditory nerve.

2. Evaluate the use of novel stimuli and electrode arrays.

3. Evaluate proposed enhancements in animals with a partially degenerated auditory nerve.

2 Summary of activities in the third quarter

In our third quarter (April - June, 1997), we collected additional electrically evoked compound action potential (EAP) data from one guinea pig and four cat preparations. We also collected additional single-fiber data from three cats; the single-unit data will be featured in this progress report. We also:

- Continued development of new data collection software to improve collection and allow real-time analysis of single-unit data. For greater efficiency, we are now developing a networked approach to data collection, i.e., acquiring data on a "slave" personal computer and performing computationally intensive analysis on a Silicon Graphics workstation.

- Were granted a renewal from the San Diego Supercomputer Center for 1000 hours of Cray computation time through June, 1998.

- Received an NIH subcontract of an SBIR grant to Advanced Bionics to test proprietary electrode designs with chronically implanted cats. After 4-to-8 week survival periods, we will obtain electrophysiological measures from the cats using these electrode arrays. The experiments

will address some of the spatial-interaction questions central to this project.

- Hosted a visit by Blake Wilson and Chris van den Honert, who provided useful insights on our data and procedures.

- Improved execution processes for modeling on the Cray. Model results are now stored in the same file format as experimental recordings. New routines now allow us to manipulate model parameters and submit multiple Cray jobs for batch execuation from our local SGI. This allows us to vary and analyze parametric effects more rapidly.

- Continued testing the approximate model solution and comparing it to the exact soluation.

- Submitted one publication (Rubinstein) and are preparing three others (Rubinstein, Miller, and Matsuoka), based upon work related to this project.

3   Single-fiber response properties: Group trends

3.1   Methods

The data presented in this report were obtained from eight cats; in all cases, stimuli were presented through an intracochlear, monopolar ball electrode inserted in basal turn to a depth which placed the ball just within the plane of the round window. In most preparations, the return electrode was positioned on the floor (i.e., ventral aspect) of the bulla; in cats beginning with C24, it was positioned in the front forepaw. The stimulus was a monophasic rectangular current pulse with a nominal duration of 20 μs. Our stimulator's bandwidth limitations, however, yielded an effective pulse duration of 26 μs, measured at the 50% amplitude points. Stimulus level was corrected by reporting the level of an ideal 26 μs rectangular pulse delivering the same charge. Anodic and cathodic pulses were delivered in an interleaved fashion with a 30 ms interval between each pulse; thus, the interval between successive pulses of the same polarity was 60 ms.

Recording electrodes were made using 1.0 mm diameter glass using a Narishige puller and 3 M KCl solution. Electrode impedances were at least 15 MΩ; improved pulling technique (using air-jet cooling) with the later preparations resulted in electrode with minimum impedances greater than

20 MΩ. Single-fiber potentials were amplified by an Axon Instruments head-stage and Axoprobe amplifier. Waveforms were acquired digitally at 100,000 samples/s with 16-bit resolution. All recordings were stored to disk, enabling us to perform offline analysis of subtle features of the neural potentials, in addition to standard peak detection. Further methodological details were included in the first quarterly progress report [1].

Figure 1 provides an example of the basic measures obtained from a series of recordings made from one fiber; in each graph, data for anodic and cathodic stimuli are plotted versus stimulus level. In the top graph, firing efficiency (FE) data are plotted. From these data threshold Th, that is, the stimulus level yielding a firing efficiency of 50%, is computed. As will be seen, the fact that anodic threshold is greater than cathodic threshold is typical of cat fibers. Fit to these input-output data are solutions to an integrated gaussian function. Note that this function fits the experimental data well. Relative Spread, RS, is then computed as defined by Verveen[12]:

$$RS = \frac{\sigma}{Th}$$

where Th is the stimulus current at a 50% firing efficiency and σ is the standard deviation of the integrated gaussian fit. RS is therefore a unitless measure of the stochastic nature of the nerve fiber and indicates the dynamic range over which the fiber can encode changes in stimulus intensity. RS values for this fiber are both about 3.5%. As discussed in the previous progress report, data we have collected suggest it may be possible to manipulate this intrinsic membrane noise by careful selection of stimulus parameters. Such manipulation could enhance the encoding of speech stimuli by cochlear implant signal processors.

The middle graph plots mean spike latency versus stimulus level. As has been reported by van den Honert and Stypulkowski[11], spike latency decreases with increasing stimulus level. Note that latency decrements also occur over levels at which firing efficiency is 100%. Reductions in latency may be due to concomittant decreases in jitter (i.e., standard deviation of spike latencies), as is suggested in the bottom graph. However, as will be seen below, latency decrements can also be caused by factors other than spike timing uncertainty.
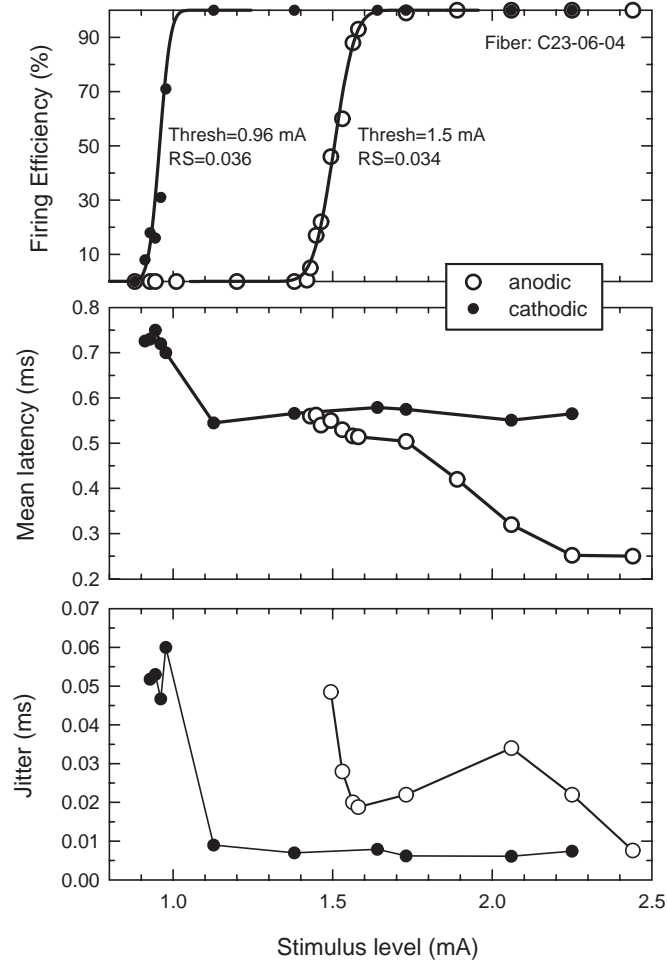
Figure 1: Input-output functions for a typical single fiber, C23-06-04. Plotted versus stimulus level are firing efficiency, mean latency, and jitter. Responses were evoked using a brief (26 μs), monophasic stimuli delievered through a monopolar electrode. Data obtained with anodic stimuli are plotted with open symbols; ca-thodic data are plotted with filled symbols. The smooth curves in the top graph are least-squared-error fits to an integrated gaussian. The minimum values for jitter may be biased upward by bandwidth limitations of our acquisition system.

3.2   Group data

Just as threshold is defined by the 50% FE point, latency and jitter can also be characterized by their values at which FE is 50%. This is done in Figure 2, where threshold, latency, jitter, and RS are summarized across single-fiber data obtained from 7 cats. At the right of each graph are plotted mean values for each measure. Two stimulus polarity effects are evident in the group mean data. First, cathodic thresholds are significantly lower than anodic thresholds (paired t-test, T = 5.42, p < 0.001, d.f. = 51) and cathodic latencies at threshold are greater than anodic latencies (paired t-test, T = 12.4, p < 0.001, d.f. = 19). Both of these trends agree with those we reported [1] in parallel measures of the electrically evoked compound action potential (EAP). For example, the EAP threshold difference across polarities is about 1.5 dB, compared to the 1.4 dB mean difference observed in the single-fiber data. No clear polarity effects are observed in the jitter or relative spread data, although there are relatively less paired data for the latter measure. Anodic and cathodic RS values are, on average, 6.9 and 6.4%.

Comparisons of these finding with previously published work are limited due to differences in stimulus parameters. Javel [4] demonstrated similarly sloped rate-level curves; however, sinusoidal or biphasic pulse trains delivered through bipolar electrodes were used. More fundamental measures were obtained by van den Honert and Stypulkowski [11] using monophasic, cathodic, stimuli delivered through a monopole. The data presented by them were important, among other reasons, in that they suggested both distal and proximal axonal processes were electrically stimulable. That hypothesis was based upon lesions to the nerve that resulted in altered single-fiber latency distributions, as well as their observation of double-peaked ("N1/N0") EAP waveforms [10]. The most comparable data were collected by Dynes (personal communication) who used 100 μs monophasic pulses via a monopolar electrode. In 13 fibers in which RS was measured for both stimulus polarities, anodic RS values ranged from 1 to 10%, while cathodic RS values ranged from 3 to 15%. No systematic polarity effect on RS was reported.

Previous findings from this research project [7] have shown that the gross neural (i.e., EAP) response demonstrates a dependence on stimulus polarity consistent with the single-fiber data reported here. While the EAP polarity effect suggests the existence of different sites of action potential initiation, the single-fiber data presented here is more compelling. The latency difference shown in here is consistent with the notion that cathodic stimuli can
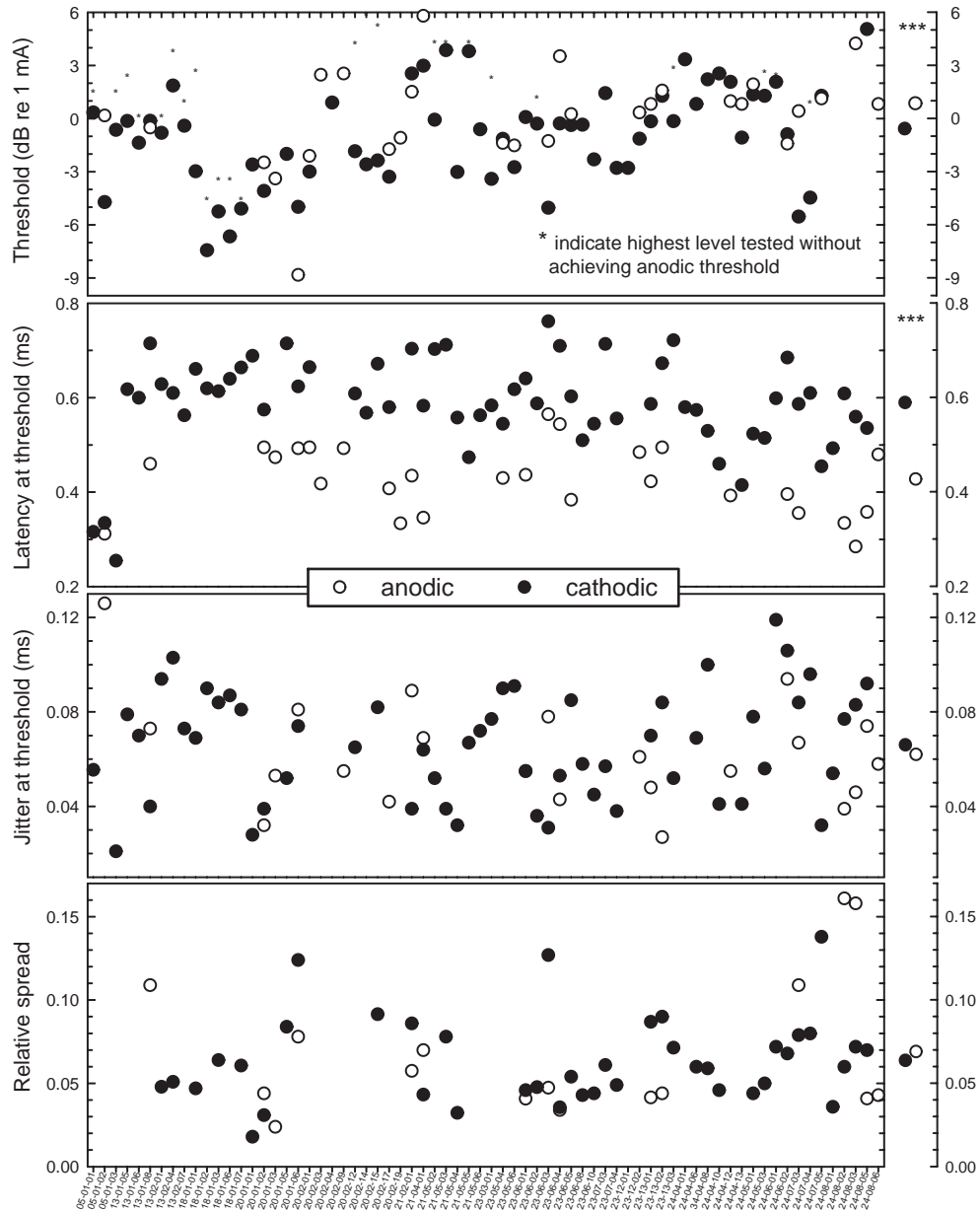
Figure 2: Summary data for single fibers from 7 cats. Threshold, latency, and jitter measures are all measured at the 50% FE level. Mean values are plotted to the right of each large graph for both stimulus polarities. Differences between anodic and cathodic mean data are statistically significant for threshold and latency (see text). Note that mean anodic threshold was computed using the "highest level tested" data.

excite more peripheral sites than does anodic stimuli. Assuming the validity of constructs such as Rattay's [8] activating function, the polarity effect on threshold may also shed light on the relative locations of the stimulating electrode and cathodic and anodic sites of excitation on single fibers.

4 Single-fiber response properties: Additional observations

Although extending our understanding of neural excitation, the response properties presented above provide only a partial picture for several reasons. A larger sample size is needed for greater confidence. Additional measures surveying likely spatio-temporal interactions await our attention. Finally, we have observed single-fiber response patterns in relatively small numbers that resist characterization by group measures but deserve mention nonetheless. In this section, we present several single-unit findings that, while not systematically observed across fibers, provide insight into excitation processes of mammalian auditory nerve fibers.

4.1 Action potential degradation

In a few of the single-fiber records examined, we occasionally observe action potentials of diminished amplitude, increased latency, and increased width. Figure 3 illustrates an example of this phenomenon, which may represent action potentials near the state of propagation failure.

At this point, we do not know the cause of this degradation. While, it may simply reflect an abnormal fiber, it may also be the result of mechanical trauma from the recording pipette. Alternatively, our evoking stimulus may put the fiber in a relative refractory state. Future planned experimental manipulations of stimulus pulse rate may clarify this issue. Finally, we note that model simulations show similar effects under conditions where spike failures occur.

4.2 Polarity-dependent threshold elevation

The threshold data of Figure 2 include fibers that failed to achieve threshold firing efficiency with anodic stimulation. Indeed, the mean anodic threshold reported above is biased downward since the "highest level tested" data (see Figure 2, top graph) were included in the estimate of the mean. Over the course of data collection, some fibers from two cats (C24, four fibers;
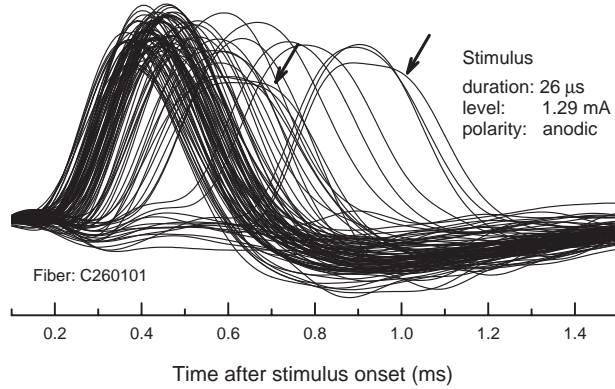
Figure 3: Example of abnormal action potentials. Arrows point to spikes with increased width and decreased amplitude. Waveforms were low-pass filtered with a 50-tap FIR filter (cut-off frequency: 5 kHz) after acquisition.
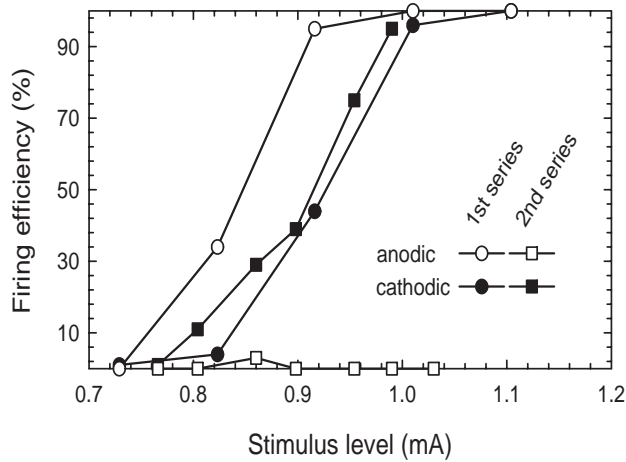

Figure 4: Example of polarity-dependent threshold elevation. Two sets of input-output functions, obtained from fiber C24-06-02, are shown. Data of the 2nd series were acquired one minute after collecting the 1st series.

C26, two fibers) exhibited threshold increases to anodic stimulation without concommittant shifting of thresholds for cathodic stimulation. An example of this behavior is shown in the repeated FE-versus-level plots of Figure 4

The mechanism underlying this adaptive behavior is unclear. As in the case of the aforementioned latency data, its dependency on stimulus polarity suggests that each polarity excites fibers in a different mode, presumably by initiating action potentials at different sites having differing membrane properties. Preliminary EAP data collected from cats suggest that there may be a small decrement in EAP amplitude resulting from presentation of stimuli at our standard interstimulus interval of 60 ms. This decrement has been observed at low stimulus levels when EAP amplitude is small compared to its maximum (saturation) amplitude. Our single-fiber data exhibiting upward threshold shifts may underlie the observed EAP decrement; further experiments will be conducted at both the gross-potential and single-fiber level to assess possible effects of stimulus pulse rate on neural adaptation properties.

4.3   Repetitive firing

A more novel finding is fibers that produce a second action potential within 1 to 2 ms after generation of an action potential with typical latency characteristics. This response has been observed in nine fibers from two cats; an example is shown in Figure 5. A characteristic of these fibers is that a spike at the later time interval occurs only if an earlier spike was produced. Repetitive firing can occur with both stimulus polarities. Two of the three fibers exhibiting double-spiking for both polarities show the temporal firing pattern illustrated in Figure 5; that is, a relatively greater time interval between the first and second spike groups for anodic stimulation.

The temporal aspect of this repetitive firing is interesting particularly in light of the model single-fiber and experimental EAP findings reported last quarter [9]. We noted that EAP amplitude-level functions for the second response of a two-pulse stimulus were susceptible to increases in slope (or RS) when the pulses were presented at an interpulse interval near 1.1 ms. Consistent with this finding, modeled fibers also underwent a large increase in RS when pulse pairs were presented at similar interpulse intervals. These findings suggest that neural membranes of fibers in a state of relative refractoriness become transiently noisier and have altered response properties. Furthermore, Chow and White [3] recently reported model simulations in which spontaneous action potentials are generated as result of stochastic ion
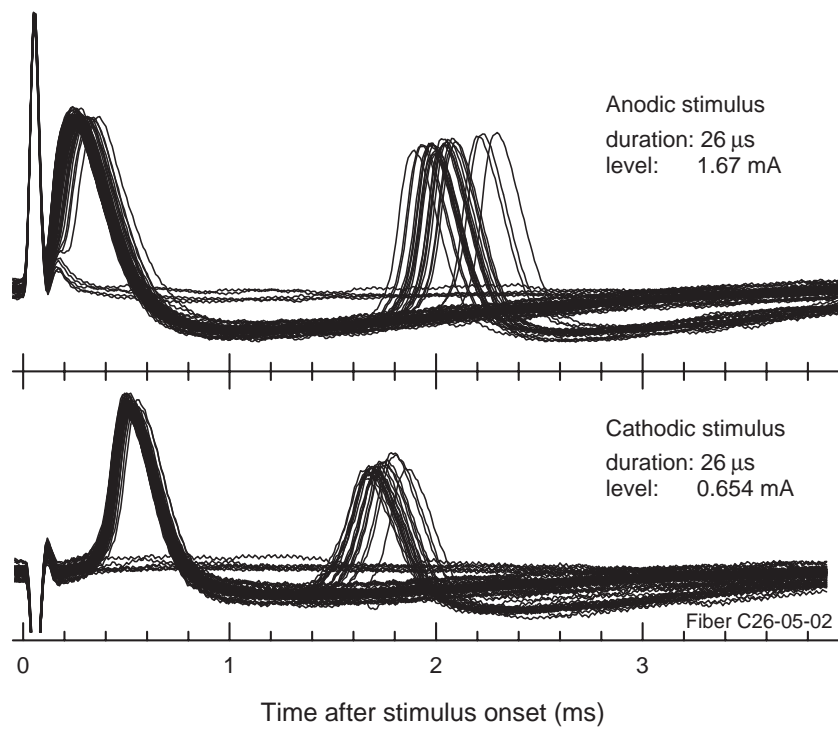
Figure 5: Example of a single fiber exhibiting repetitive firing. The stimulus artifact is seen between 0 and 0.2 ms in each trace.
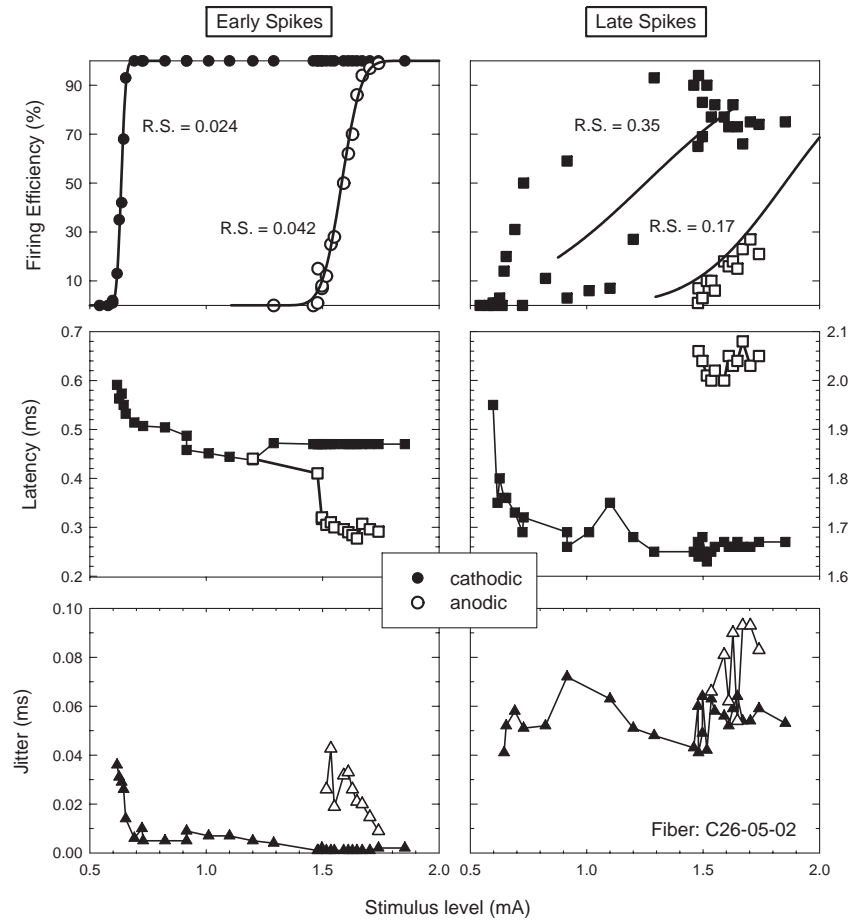
Figure 6: Input-output properties of a fiber with repetitive firing. Data describe the same fiber shown in the previous figure.

channel dynamics.

The repetitive firing noted here may be another manifestation of increased membrane noise resulting from the presentation of a prior stimulus. In this case, however, fibers may be capable of generating a second action potential spontaneously as a consequence of greatly elevated membrane noise. The input-output and temporal statistics of the unit shown here is consistent with this notion (Figure 6). Firing efficiency, latency, and jitter versus stimulus level are shown for the early (i.e., normal) set of spikes in the graphs of the left column; data for the second (later) set of responses are shown in the right column.

Note that while the firing efficiency functions are typical for the early set, the range of stimulus levels over which the second set of spikes respond probabilistically is much greater. Also, the jitter of the later group of spikes is, at all stimulus levels, greater for than that of the early group. Both of these trends suggest that the initiation site of the later set of action potentials is noisier.

4.4   After-hyperpolarization

The acquisition and disk-storage of single-fiber waveforms enables us to examine aspects of the neural response beyond that afforded by standard spike timing analysis. The responses of fiber C26-05-02, for example (Figure 5), clearly show after hyperpolarization for a period of about 2 ms after depolarization. Observation and measurement of this recovery phase is important for accurate model simulations of auditory nerve fibers since it suggests the operation of potassium channels at the nodes. As a result of this observation, we will run simulations of this potential by incorporating a delayed rectifier to the model node of Ranvier.

4.5   Bimodal post-stimulus time histograms

Studies by van den Honert and Stypulkoswki [10],[11] provided evidence based primarily upon EAP measures that both the peripheral and proximal axonal processes of auditory nerve fibers may be action potential initiation sites. Others have also observed complex gross-potential morphologies consistent with the hypothesis that two types of single-unit responses may contribute to the gross potential [6]. A difficulty with the multiple intiation-site hypothesis was that no direct single-fiber data were available to corroborate that interpretation of the EAP measures. As such, it was unclear whether

single fibers possessed two response modalities or that the observed complex EAP morphology was due to two subpopulations of single fibers, each responding in one mode.

We have observed single-fiber responses from four fibers of four cats that are consistent with the two-site hypothesis in that they demonstrate a discrete, level-dependent decrement in latency. Of those fibers, systematic data from two have been collected and are presented below (Figure 7). In both cases, the evoking stimulus was a 26 μs monophasic pulse delivered to a monopolar electrode located in the basal turn of the cat cochlea. The poststimulus time histograms of fiber C23-06-01 (Figure 7, left column) were obtained using cathodic stimuli; those of fiber C26-07-07 (right column), were collected using anodic stimuli.

In both cases, the histograms exhibit a level-dependent, bimodal distribution of latencies. As stimulus level is increased, each fiber first achieves a firing efficiency of 100% with all spikes occuring at the longer latency locus. With further increases in level, a second locus of latencies develops at a shorter latency. At sufficiently high stimulus levels, the fiber responds 100% of the time at that locus. Indeed, in all the panels of Figure 7, both units are responding at 100%.

There are insufficient data in the input-output function of fiber C23-06-01 to obtain an accurate estimate of RS; however, sufficient data were collected from fiber C26-07-07 to perform meaningful analyses. The top graph of Figure 8 shows firing efficiency versus stimulus level for both the long and short latency spike groups (filled and open symbols, respectively). In the top graph of FE versus level, note that as stimulus level is increased beyond 2.1 mA, there is a perfect trade-off between the firing efficiency of the late-latency and early-latency response modes. Also, the estimates of the underlying integrated gaussian functions fit the data very well. The calculated values of RS for the "late" and "early" modes are 4.4 and 1.65%, respectively; 95% confidence intervals for these two estimates are (4.1 - 4.7%) and (1.35 - 1.8%), respectively. Thus, the two response modes differ in threshold, latency, and RS in a manner consistent with the hypothesis that two different longitudinal sites of auditory nerve fibers are stimulable and that they have measurably different electrophysiological properties. The fact that there is a discrete shift in latency between the two modes is consistent with the notion that a unstimulable region of the fiber – such as the cell body – is interposed between the two excitation sites. Finally, the two distinct values of RS are consistent with the differential anatomy of the distal and proximal cat axons [5] and the putative relationship between axon diameter
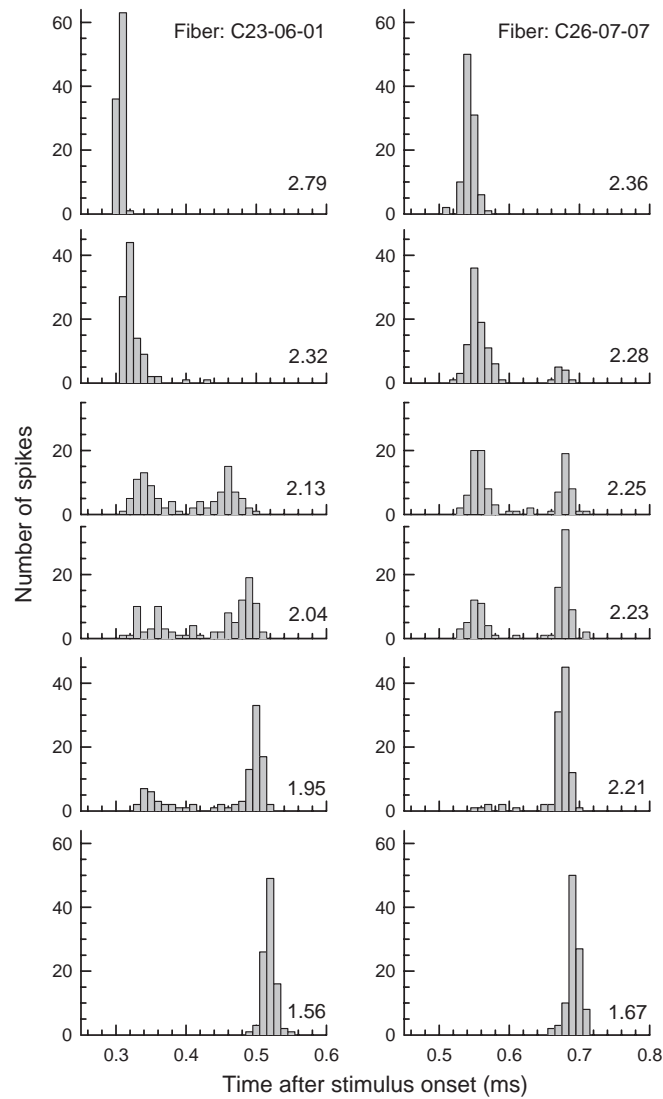
Figure 7: Single-fiber histograms with bimodal distributions. Histograms obtained at various stimulus levels are shown for two fibers. The parameter in each graph indicates stimulus level in milliamperes.
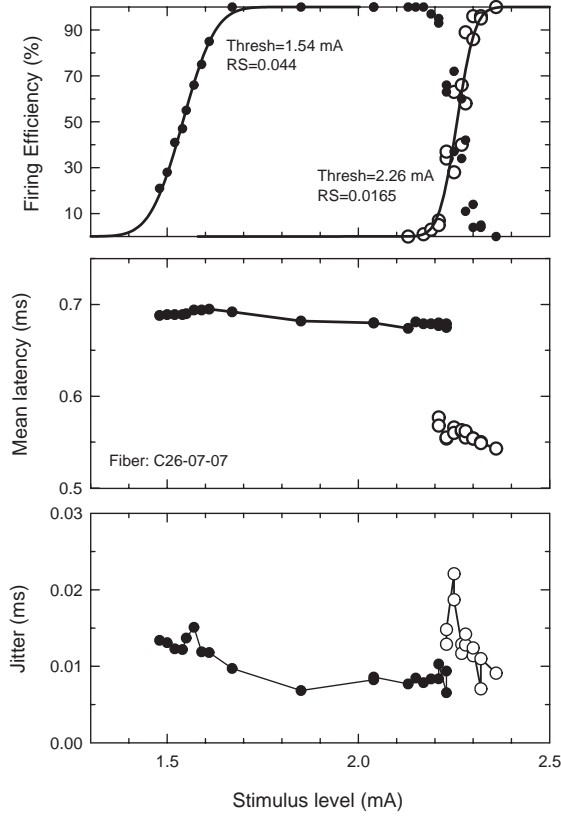
Figure 8: Input-output characteristics of fiber C26-07-07, which exhibited a bimodal histogram (see previous Figure, left column). Data describing spike activity occurring at low stimulus level (i.e., longer latency spikes) are shown in filled symbols; open symbols describe shorter-latency spikes occurring at higher stimulus levels.

and RS [13].

Other aspects of these responses are worth noting. For fiber C26-07-07, anodic stimulation yielded a bimodal response pattern; however, cathodic stimulation produced a unimodal histogram with a most probable latency ranging from 0.60 to 0.56 ms, corresponding to the earlier of the two bimodal peaks. If our conjectures are true, then in this case, anodic stimuli can excite membrane on either side of the cell body, whereas cathodic stimuli excites only the proximal site. Note also that in the case of fiber C23-06-01, the bimodal distributions occur at relatively short latencies. It is possible that the absolute latency difference observed between the two fibers reflects underlying differences in length among feline auditory nerve fibers [2]. Differences in the position of the recording electrode may also contribute to the latency offset.

Finally, these responses have only been observed in a minority (about 5 - 10%) of fibers encountered. Our EAP waveforms, unlike those reported by Stypulkowski and van den Honert [10], rarely appear as double-peaked ("N1/N0") potentials; suggesting that a only small fraction of fibers produce this bimodal pattern, at least in a highly synchronized fashion. Given the complex pattern of fiber orientations in the mammalian cochlea, it is not surprising that we have encountered a heterogeneous pattern of single-fiber responses. Clearly, we need to collect a larger sample of fibers in order to characterize auditory nerve fiber responses to our basic electrical stimuli.

5 Summary

Of the three project goals listed in the Introduction, the first is addressed by the data reported here. Preliminary findings of an ongoing survey of fiber response properties were presented. Using relatively simple stimulus delivery (i.e., 26 μs monophasic pulses via a monopolar intracochlear electrode), we observed the following:

1. Relative to anodic stimuli, cathodic current pulses evoke responses at lower stimulus levels and yield histograms with longer mean latencies.

2. The mean value for relative spread (RS) is 6.9 and 6.4 %, for anodic and cathodic stimuli, respectively. No systematic effect of stimulus polarity was observed for RS or jitter.

3. In some cases, fibers respond more than once to a single pulsatile stimulus. We speculate that this may be due to greatly enhanced

membrane noise facilitated by previous firing and may relate to the effects of stimulus pulse rate discussed in the previous progress report.

4. A few fibers produce bimodal histograms and input-output properties consistent with the hypothesis that both the proximal and distal axonal processes may be electrically stimulable and respond in measurably different ways.

6   Plans for the fourth quarter of this project

The following activities are planned for the fourth quarter (July - Septempber, 1997) of this research project:

- Continue and extend studies of cat single-fiber responses, with emphasis on characterizing responses to stimuli presented at different interpulse intervals and obtaining data from larger populations of fibers from each cat.

- Begin collection of EAP data from cats using multiple-electrode intracochlear arrays for stimulation to assess channel-interaction effects.

- Further software development for single-fiber data acquisition using the aforementioned networked, two-computer approach. Across-computer communications protocols will be written, debugged, and completed, as will initial testing of data acquisition routines.

- Begin studies of chronically implanted cats using experimental electrode arrays fabricated by Advanced Bionics. Five cats will be implanted with functional and nonfunctional arrays. After survival periods of 4 to 8 weeks, they will be sacrificed for histological surveys of the cochlea and auditory nerve. Also, electrophysiological measures will be obtained using the functional arrays immediately prior to sacrifice.

- Host consulting visits by Don Eddington and Blake Wilson.

- Four podium and poster presentations will be given by the authors on various aspects of this project at the Conference on Implantable Auditory Prostheses, August 16-21, Pacific Grove, California.

- Effort will be made to submit at least two papers based on material in the first two progress reports.

References

[1] Abbas, P.J., Rubinstein, J.T., Miller, C.A., and Matsuoka, A.J. (1997). The neurophysiological effects of stimulated auditory prosthesis stimulation [First quarterly progress report, NIH grant N01-DC-2111]

[2] Arnesen, A.R. and Osen, K.K. (1978). The cochlear nerve in the cat: topography, cochleotopy, and fiber spectrum. *J. Comp. Neur.*, 178, 661-678.

[3] Chow, C.C. and White, J.A. (1996). Spontaneous action potentials due to channel fluctuations. *Biophys. J.*, 71, 3013-3021.

[4] Javel, E., Tong, Y.C., Shepherd, R.K., and Clark, G.M. (1987). Responses of cat auditory nerve fibers to biphasic electrical current pulses. *Ann. Otol. Rhinol. Laryngol.*, 96 (Suppl. 128), 26-30.

[5] Liberman, M.C. and Oliver, M.E. (1984). Morphometry of intracellularly labeled neurons of the auditory nerve: correlations with functional properties. *J. Comp. Neurol.*, 223, 163-176.

[6] Miller, C.A., Abbas, P.J., and Robinson, B.K. (1993). Characterization of wave I of the electrically evoked auditory brainstem response in the guinea pig. *Hear. Res.*, 69, 35-44.

[7] Miller, C.A., Abbas, P.J., Matsuoka, A.J., and Rubinstein, J.T. (1997). A comparison of the electrically evoked compound action potential from guinea pig and cat using monophasic anodic and cathodic pulsatile stimuli. *Assoc. Res. Otolaryngol. Abs.*, 224.

[8] Rattay, F. (1987). Ways to approximate current-distance relations for electrically stimulated fibers. *J. Theor. Biol.*, 125, 339-349.

[9] Rubinstein, J.T., Matsuoka, A.J., Abbas, P.J., and Miller, C.A. (1997) The neurophysiological effects of stimulated auditory prosthesis stimulation [Second quarterly progress report, NIH grant N01-DC-2111].

[10] Stypulkowski, P.H. and van den Honert, C. (1984). Physiological properties of the electrically stimulated auditory nerve. I. Compound action potential recordings. *Hear. Res.*, 14, 205-223.

[11] van den Honert, C. and Stypulkowski, P.H. (1984). Physiological properties of the electrically stimulated auditory nerve. II. Single fiber recordings. *Hear. Res.*, 14, 225–243.

[12] Verveen, A.A. (1961). *Fluctuation in Excitability*, Drukkerij, Holland N.V., Amsterdam.

[13] Verveen, A.A. (1962). Fibre diameter and fluctuation in excitability. *Acta Morphol. Neerland. Scand.*, 5, 79-85.